TREE-RING RESEARCH, *Vol. 71(1), 2015, pp. 25–36*
DOI: http://dx.doi.org/10.3959/1536-1098-71.1.25

HOW TO IMPROVE DENDROGEOMORPHIC SAMPLING: VARIOGRAM ANALYSES OF WOOD DENSITY USING X-RAY COMPUTED TOMOGRAPHY

CAROLINA GUARDIOLA-ALBERT[1]*, J. A. BALLESTEROS-CÁNOVAS[2,3], M. STOFFEL[2,3], and **A. DÍEZ-HERRERO[1]**

[1]Geological Survey of Spain, Ríos Rosas 23, E-28003 Madrid, Spain

[2]Laboratory of Dendrogeomorphology, Institut of Geological Sciences, University of Berne, Baltzerstrasse 1+3, Berne, Switzerland

[3]Climatic Change and Climate Impacts, Institute for Environmental Sciences, University of Geneva, 7, chemin de Drize, CH-1227 Carouge-Geneva, Switzerland

ABSTRACT

Knowledge of the spatial heterogeneity of wood is useful for industrial applications and improving dendrogeomorphic sampling, because it allows a better understanding of 3-D wood density structure in tree stems damaged by geomorphic processes. X-ray computed tomography (XRCT) scanning as a means of non-destructive measurement has become an important technique in tree research as it allows the detection of internal variations in wood density. In this paper a new methodology for modelling spatial variations of relative wood density using variograms on XRCT images is developed. For each tree, XRCT images perpendicular to the stem axis were obtained with 1-mm spacing. In a first step, ImageJ software was used to process each image. Then, more than 30 one-dimensional variograms were studied for a selected number of cross-sections. The results show that there is a pattern in the diffusion of relative wood density linked to the attenuation of the geomorphic damage along the stem from the wounded area. Although the number of samples could be increased, these preliminary results demonstrate that variograms of XRCT are a useful tool to optimize dendrogeomorphic sampling, saving time and costs.

Keywords: flash floods, tree rings, variogram analysis, wounds, wood density, X-ray computed tomography.

INTRODUCTION

Wood is a natural material characterized as anisotropic and heterogeneous because of the complexity of its orthotropic biological structure formed by different types of cells (García-Esteban *et al.* 2003). The factors that modulate this heterogeneity of wood are genetically related and usually stable in the medium term; but they are also linked to environmental or external factors, which can vary in the short term and are responsible for the adaptive capacity of trees (Schweingruber *et al.* 2006). It has therefore been widely reported that environmental and external factors induce anatomical changes in wood structure (Garcia-Gonzalez and Fonti 2006; Stoffel and Hitz 2008), and may even trigger loss of wood quality and decay stages in the tree (Shigo 1984; Smith and Sutherland 1999; Romero *et al.* 2009).

The analysis of wood properties is essential to improve efficiency in the wood industry (Castell *et al.* 2005), but it also plays an important role in environmental sciences (Schweingruber *et al.* 2006; Stoffel *et al.* 2010). It has been shown that the wood structure (*i.e.* tree rings) can provide proxy information about past climatic dynamics and several environmental processes (Fritts 1976; Fonti *et al.* 2007; Arbellay *et al.* 2014). Specifically, the analysis of wood density structures has been demonstrated to be of major importance in

*Corresponding author: c.guardiola@igme.es; Fax: +34 91 442 6216; Telephone: +34 913495829.

dendrochronology and related sciences (Schinker *et al.* 2003), where it has been used to reconstruct the past temperature regime (Fan *et al.* 2009), to understand the ecophysiology of trees (Arbellay *et al.* 2012), and to detect past geomorphic events (Arbellay *et al.* 2010; Ballesteros-Canovas *et al.* 2010a, 2010b; Stoffel and Bollschweiller 2010). Anatomical changes in conifer trees typically include suppressed ring width and significant reduction in earlywood tracheid size (Stoffel and Hitz 2008), in addition to tangential rows of traumatic resin ducts formed around wounds (Schneuwly *et al.* 2009a, 2009b). Responses of broadleaved trees to flood disturbance can vary significantly between species, but substantial decreases in vessel size have been described as the foremost common response (Arbellay *et al.* 2012).

New advances in non-destructive methods have been shown to be very successful in the analysis of three-dimensional wood characteristics (Bhandarkar *et al.* 1999; Longuetaud *et al.* 2005; Stoffel and Klinkmüler 2013; Van den Bulcke *et al.* 2014). In this context, XRCT scanning is one of the most powerful tools. The pixel grey-level in a XRCT image represents the X-ray attenuation coefficient, which is proportional to the amount of X-ray energy absorbed and consequently the average density of the material within the 3-D volume representing that pixel (Freyburger *et al.* 2009). Lower (higher) material densities will thereby result in lower (higher) grey-level pixel values in the XRCT image. However, grey-level values may also be affected by moisture, temperature and the phytosanitary state (Bhandarkar *et al.* 1999).

The earliest XRCT scanners were developed for medical use in the early 1970s, whereby measured X-ray absorption was correlated with material density. The first studies for internal stem defects started in the 1980s (*e.g.* Benson-Cooper *et al.* 1982; Funt and Bryant 1985, 1987; Roder *et al.* 1989; Wagner *et al.* 1989; Hodges *et al.* 1990; Chang 1990). Since then it has been demonstrated that XRCT scanners can be used successfully to image the internal features of trees (Bhandarkar *et al.* 1999; Longuetaud 2005). Based on visual comparison of crosscut stem sections with the corresponding XRCT images, it was demonstrated that defects can be identified in images (Stoffel and Klinkmüler 2013). Considerable efforts have been made ever since to develop new algorithms to analyze wood density variations (Leban *et al.* 2004) and to identify stem defects and clear wood, as well as to perform 3-D reconstruction of the stem sample. In dendrochronologic studies this application of XRCT is valuable to determine changes in the wood structure and define their dimension.

However, in order to understand spatially distributed natural variables, it is essential to estimate their geospatial structures (Chilès and Delfiner 2008). Geostatistical analysis is widely used to study the spatial variability of environmental systems (Goovaerts 1997; Webster and Oliver 2007). In a statistical context, tonal variations in the spatial domain can be described in terms of the two main conceptual components associated with pixels (or other units): variability and spatial correlation. The latter characteristic, spatial correlation, assumes that pixels are not completely randomly distributed within an image and that there is therefore a spatial variability structure associated with them. The advantage of the geostatistical approach is that both aspects can be jointly modelled (Chica-Olmo and Abarca-Hernández 2000). The variogram function summarizes the strength of associations between responses as a function of distance, and possibly direction. The variogram has been widely used for many years to quantify the spatial variability of geo-referenced phenomena (*e.g.* Journel and Huijbregts 1978; Armstrong 1984; Olea 1994; Goovaerts 1997).

The main aim of this paper is to define a methodology based on geostatistical techniques to study the 3-D density of wood structures, in order to obtain a better understanding of tree stem response to mechanical disturbance. This preliminary research therefore focuses on the definition of a methodology that uses variogram tools to analyze XRCT images of tree damage caused by flash floods.

Traditionally, dendrogeomorphic sampling involves the collection of two or three tree cores from stems extracted with increment borers. To

avoid tree damage, such sampling is usually kept to a minimum while at the same time the signal has to be maximized. This present work offers a valuable enhancement to tree sampling efficacy during dendrogeomorphic studies, and therefore extends the applicability of the methods for natural hazard studies.

MATERIAL AND METHODS

Tree Sampling

During the autumn of 2011, taking advantage of the forestry work carried out by the relevant Basin Authority (*Confederación Hidrográfica del Tajo*), 37 samples (between 86.2 and 144.6 cm in diameter) were collected from riparian trees (namely, ash or *Fraxinus angustifolia* Vahl., alder or *Alnus glutinosa* L. and willow or *Salix atrocinerea* Brot.) wounded by flood events on the floodplain of the Alberche river (Sierra de Gredos -Spanish Central System). The sampling procedure was carried out using a chainsaw and focused on the wounded stem portion. All sampled trees were adequately characterized in the field (*i.e.* position, size, dominance, number, size and position of wounds), and the samples were then stored in a dry, cool room. All the samples were then packed and sent to the Laboratory of Forensic Medicine at the University of Bern (Switzerland). For the present study, two trees (one *F. angustifolia* and one *A. glutinosa*) were selected from the 37 samples based on macroscopic inspection of all XRCT images, to retrieve high-accuracy structural information.

X-Ray Computed Tomography (XRCT)

According to Bhandarkar *et al.* (1999), different wood characteristics can be interpreted from XRCT cross-section images in trees affected by floods (Figure 1). Variations in the wood density are reflected in the grey-level distribution. Tree rings alternating layers of earlywood (*EW*) and latewood (*LW*) can be seen because *LW* is composed of smaller cells of higher density than *EW* and hence appears brighter in the XRCT images. The bark tissue surrounding the stem cross-section has a higher density because of higher moisture and inorganic material content. It can therefore be seen as a bright ring surrounding the stem. Internal holes have low density and therefore grey-levels near zero appear in the XRCT image. The callus pad (*cp*) is represented by high grey-level values and is formed by tree rings with high-density cells closing the wounds. Because decay has a decreased amount of cellulose and lignin, it has a lower density and shows up darker when compared to normal wood. However, the chemical barrier zone (*bz*) is characterized by high-density cells (high grey-levels) produced by the cambium immediately after wounding. Reaction wood (*rw*) is the response to the inclination of the tree stem, and is shown as high grey-level values because of the increased density.

3-D images were obtained with an XRCT device at the University of Bern. 701 and 645 images, respectively, were obtained of the two trees, perpendicular to the stem axis with 1-mm spacing. Image cross-sections were obtained of 512 $\times$ 512 pixels, with pixel sizes 0.386 mm for *A. glutinosa* and 0.322 mm for *F. angustifolia*. The images were quantized to 16-bit and stored in the DICOM (Digital Imaging and Communications in Medicine) format. Visualization and basic image treatments were performed using ImageJ, a public domain, Java-based image processing program developed at the National Institute of Health, USA (Abràmoff *et al.* 2004). From the large database, nine cross-sections of one *A. glutinosa* sample and five cross-sections of one *F. angustifolia* sample were selected as representative of the scars. Within each cross-section 1-D pixel value profiles were digitally sampled from pith to bark making a radial sweep from 0 to 360°. For *A. glutinosa*, 43 1-D profiles per cross-section were sampled, whereas 36 were taken for *F. Angustifolia* slices.

Spatial Variability of Wood Density

The spatial variability of the wood density was analyzed with variograms (Matheron 1965; Isaaks and Srivastava 1989; Armstrong 1998), because they allow semivariances to be plotted as a function of distance from a point. Geostatistical modelling generally uses the variogram instead of

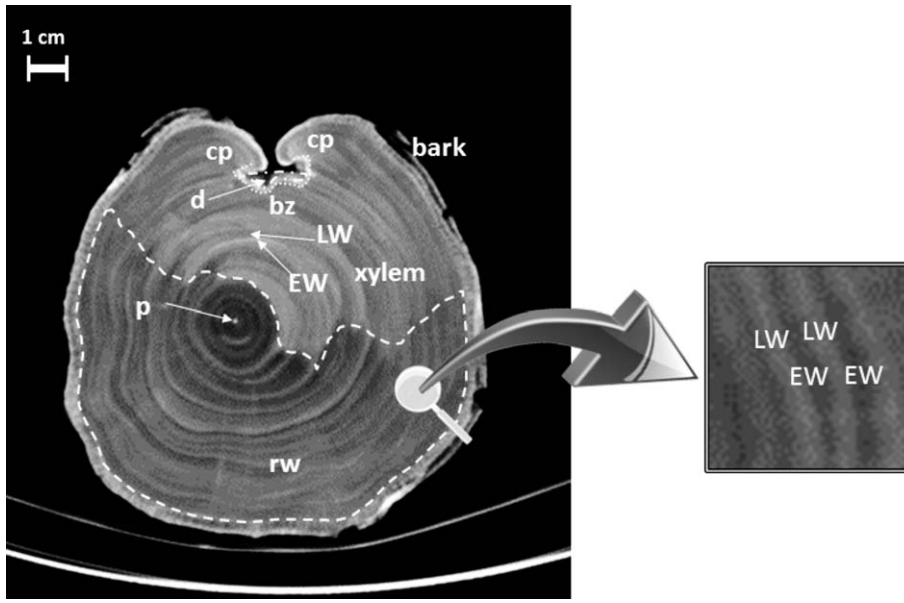

Figure 1. XRCT image reflecting different wood structures related with mechanical wounding (*bz*: barrier zone, *d*: decay, *cp*: callus pad, *rw*: reaction wood, *EW*: earlywood, *LW*: latewood, *p*: pith). For more details on the physiology of wounds refer to Shigo (1984) and Arbellay *et al.* (2012).

covariance for purely historical reasons. It is assumed that spatial autocorrelation does not depend on where a pair of observations is located, but only on the distance between the two observations, and on the direction of their relative displacement. The sill is the ordinate value at which the variogram levels off (*i.e.* its asymptotic value), equals the variance of the underlying studied population. For a given distance, homogeneous measurements result in similar sills. However, if there is a damage or change in the wood structure, the heterogeneities induced by environmental processes will be reflected in a differentiation of sill values. The range is the distance at which this levelling off occurs (*i.e.* the spatial extent of the structure in the data). The variogram is defined by

$$\gamma(h) = \frac{1}{2N}\sum_{i=1}^{N}[z(x_i) - z(x_i + h)]^2 \qquad (1)$$

where N is the number of data sample pairs separated at distance h, $z(x_i)$ are grey-level sample values and $z(x_i + h)$ are all the grey-level sample values at a distance h from the point x_i.

The wood structure of a cross-section is heterogeneous and asymmetrical, whereas the mathematical function of a variogram is symmetrical. These two facts meant that the scanned cross-sections had to be studied through 1-D raw data profiles taking values from pith to bark. 1-D experimental variograms were computed from these profiles and the computations were carried out with Gslib software (Deutsch and Journel 1992) and Excel worksheets. In this case, we avoided the use of 2-D variograms because of the asymmetry in the wood density structure. 2-D variograms average opposite directions and hence significant wood features cannot be detected (*i.e.* wounds normally appear in the direction of the impact and are absent in the opposite direction). This fact should be carefully taken into account in studies attempting to use variograms to estimate and simulate 3-D wood density structures, as proposed by Castell *et al.* (2005).

The first step was to test our hypothesis that variogram changes can provide information about flood-wounded trees. The methodology was designed to identify significant changes in the behavior of variograms from wounded and non-wounded cross-sections. In the scanned images it

is easy to identify which cross-sections are free of any mechanical damage and which ones are noticeably impacted. If the variogram in these two types of images presents different characteristics, these variogram changes will be interpreted as an indicator of the flood damage. Once this was confirmed, differences in the variogram behavior were studied to measure the extent of the damage caused by mechanical impacts. To keep the methodology as simple as possible, the variograms were not modelled and only experimental values were analysed. Similarly, differences in variograms were measured just looking at the sill and range of the experimental variograms near the origin. This decision is based on the fact that continuity and regularity in space are related to the behavior of the variogram near the origin (Journel and Huijbregts 1978).

The damage dimension, calculated in angle units from the scar location, is here defined by the angular distance of affection (A). A methodology created to automate this process made it possible to analyze a high number of cross-sections with less time/cost and therefore achieve more robust conclusions. The complete study of one specimen sample for each cross-section includes between 20 and 60 radial profiles ranging from 0° to 360°. In general, more profiles are taken in the vicinity of open and healed scars. The new approach proposed here uses the Wilcoxon non-parametric statistical test (Wilcoxon 1945) with 95% confidence level to find different statistical behaviors at the right and left ends of the scar. This statistical test establishes a systematic and objective procedure. Right and left sides were studied to analyze differences in both flanks of the scar. Left minus right angles that show different statistical behavior for the mean thereby provide an estimation of A.

RESULTS AND DISCUSSION

Resulting One-Dimensional Variograms of XRCT Images

Two of the cross-sections selected for the *F. angustifolia* specimen were studied: one uninjured and one highly injured. For both cross-sections eight profiles were digitized from the pith to the bark in the following directions: 90°, 63°, 45°, 26°, 0°, 334° and 297°. Figure 2 shows the eight directional variograms for each profile in the undamaged (Figure 2a) and damaged (Figure 2b) cross-sections. In the undamaged cross-section, the directional variograms did not show significant changes. The wood density in this cross-section shows isotropic behavior, with almost indistinguishable fluctuations. However, the behavior of the variogram in the damaged cross-section presents visible changes in each direction. Although the range does not vary, the sill depends on the experimental variogram direction. The interpretation is that the spatial dimension at which wood density is correlated is the same in all directions, but the whole variability is not visible in some of them. The 0° variogram has the lowest sill and its perpendicular direction has the highest. This anisotropy detected by the variogram can be attributed to the injuries caused in the wood structure, reflecting the direction of impact. Sills diminish when the wood density is lower, which can be caused by decay, whereas sills increase when wood gets thicker (*i.e.* as a reaction to the impact) or because of moisture increase (Bhandarkar *et al.* 1999). For this example, wood density decreases in the direction of impact as sills decrease, reflecting the loss of bark and an important reduction of the diameter after collision.

All the computed variograms in all directions are non-stationary because none of them reaches a sill (see Figure 2). Another essential characteristic is the first wave present in the variograms, which is typical of processes with cyclicity (Armstrong 1998). Here cyclicity is attributed to the circular tree rings. In Figure 2b (damaged cross-section variogram), the 90° variogram lacks cyclicity and the non-stationarity is considerably reduced. The variogram reflects the effects of the impact by not registering any cyclicity, which has been attributed to the tree-ring original structure. However, from 0° to ± 45° cyclicity is present, and thus the damage is not present within these directions. In this cross-section, the lack of cyclicity can be seen as the degree of injuries in the wood and could be used as a measure of their magnitude.

Figure 3c shows values from the experimental variogram computed within the scar of the same *F. angustifolia* specimen in four directions.

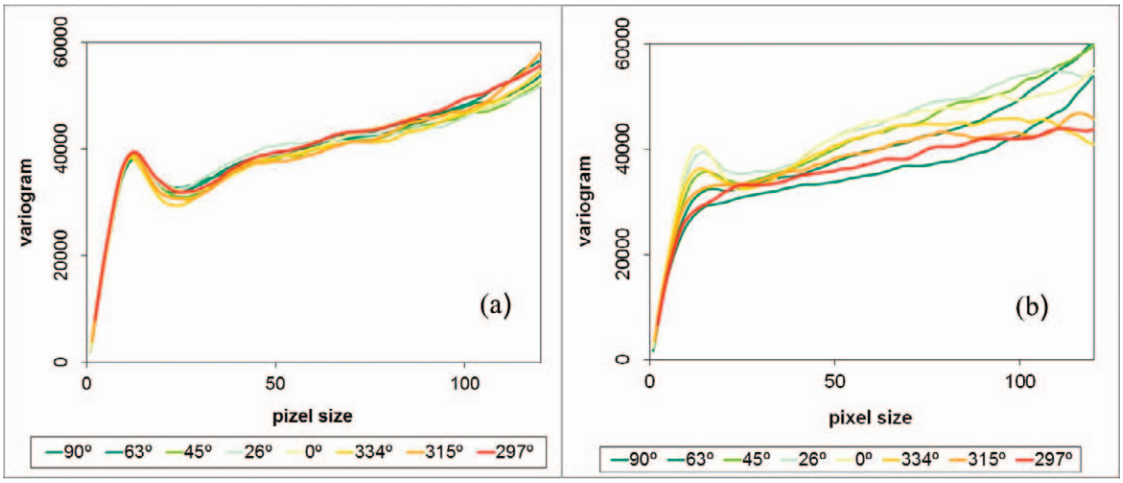

Figure 2. Directional variograms for two *F. angustifolia* cross-sections. Lag units are in pixels. (a) Undamaged cross-section. (b) Damaged cross-section.

Again, the wave behavior in the variograms reflects the presence of tree rings (cyclicity). High sills are found within the scar because thicker wood is present (*i.e.* direction a), whereas outside the scar, the variogram shows lower sill values and hence less dense wood. Direction d can be attributed to a less-affected direction: lower sill, lower density and no compaction caused by any impact (Figure 3c). Variograms in directions b and c (Figure 3a) present attenuated versions of direction d as they are not exactly in the direction of impact. It is worth noting that the range of the variogram remains fairly constant for all directions, meaning that computed experimental variograms are indeed suffering from zonal anisotropy (Isaaks and Srivastava 1989). In other words, the distance at which the wood density is correlated is the same for the different angles.

Angular Distance Affection

Once the relationship between variogram and wood density changes had been developed as explained in the previous section, the next step

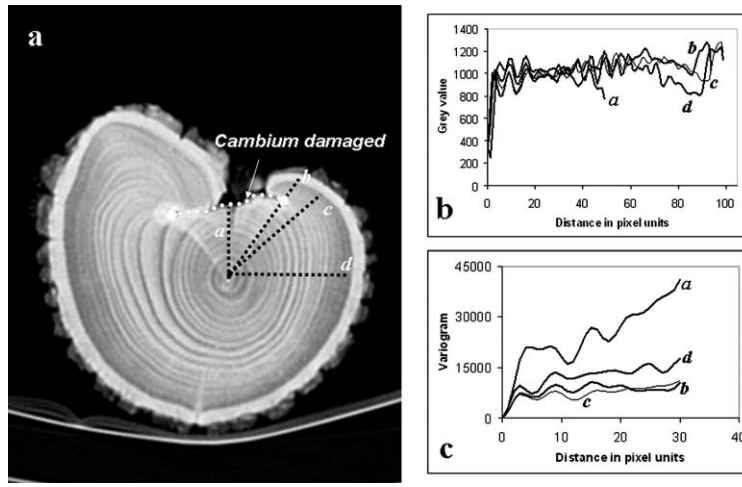

Figure 3. (a) Cross-section for one *F. angustifolia*; (b) 1-D data sampled in different directions; (c) Variograms computed in the directions shown in (b).

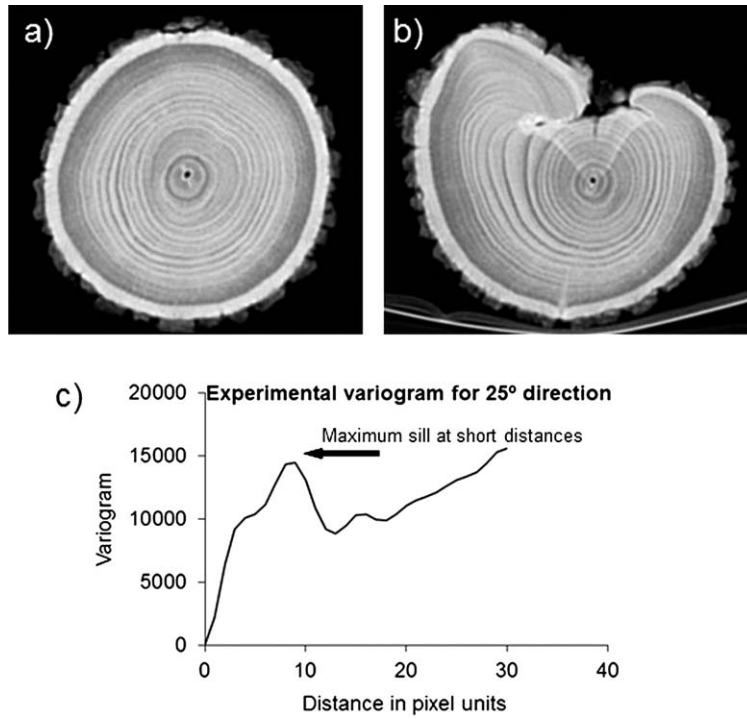

Figure 4. *A. glutinosa* cross-section images selected from (a) undamaged and (b) highly damaged sections. (c) Example of the maximum sill value at small distances.

proposed in the methodology was undertaken. As explained above, an angular distance of affection (A) was defined to measure the extent of damage caused by mechanical impacts and both sides of the scar were considered. First, to show how A values were computed, the same two cross-sections analyzed in Figure 2 were used (Figure 4a and 4b).

An estimation of the angular distance affection A in trees can be obtained by measuring the angular sector within which the maximum sills of the experimental variograms are considerably different from and higher than the ones computed on undamaged cross-sections.

The radial plot illustrated in Figure 5 shows clearly that sills increase close to the scar in the damaged cross-sections. For undamaged cross-sections, sills at small distances in the variogram remain almost unchanged. In this radial plot it is easy to determine visually the angular distance affection A. Between 10° and 175° the computed maximum sills are considerably dissimilar, therefore $A \approx 165°$. This result reveals that the affected area within the wood is wider than the internal scar area visually identified on the scanned image (*i.e.* 40° and 35° wider to right and left, respectively).

These simple visual examples show how well the proposed approach works and the potential interpretations that experimental variogram computations can provide. But it is essential to go further and perform a complete study of the specimens sampled. Different trees present diverse features depending on the height of the location of the cross-sections and on the different physiological reactions to mechanical impact (*e.g.* changes in tree-ring sizes, moisture content, inorganic minerals, internal holes, callus pad, reaction to wood invading organisms). Next, two complete studies for the selected specimens of two different species (*A. glutinosa* and *F. angustifolia*) are discussed. Nine cross-sections of *A. glutinosa* and five cross-sections of *F. angustifolia* were selected as representative of the scars. The 1-D radial profiles were digitally sampled at 43 and 36,

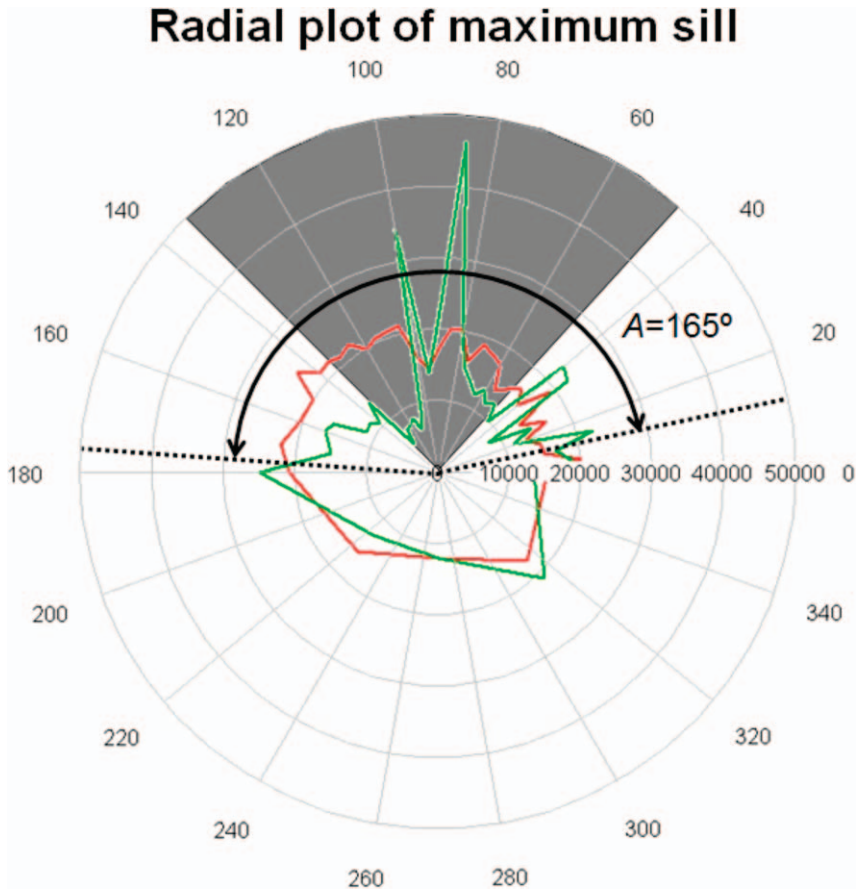

Figure 5. Radial plot of maximum sills at small variogram distances for the two cross-sections shown in Figure 4. The grey area represents the internal scar dimension in angles. The red line is the maximum sills for the undamaged cross-section. The green line corresponds to the maximum sills measured in the damaged cross-section.

respectively, for each *A. glutinosa* and *F. Angustifolia* cross-sections. More profiles were taken in the vicinity of the scar. 1-D variograms were systematically computed for each sampled profile and the maximum sill near the origin of the variogram was recorded.

In the first example the A value was calculated based on the visual comparison of sill fluctuations with the angle of the profiles/variograms. But now the proposed methodology uses Wilcoxon tests to compare the statistical behavior of the sill values to ensure a systematic procedure, to reach robust and objective conclusions. Wilcoxon test results for each of the studied cross-sections are summarized in Table 1. For *A. glutinosa*, the mean value of A is equal to 181°, indicating that the affection attributed to the injury can be classified as medium to high. Macroscopic analysis reveals the presence of a closed (healed) scar that was produced in 1997. In the case of the *F. angustifolia* the mean value of A is equal to 82°. According to this value the impact would be classified as medium. Here macroscopic analysis also points to a closed scar produced in 2002.

Improving Dendrogeomorphic Sampling

Injuries have to be sampled with at least one core per scar, with cores extracted from the overgrowing tissue at the height showing the maximum wound extension (Schneuwly *et al.*

Table 1. Calculation of the Angular Distance Affection (*A*) for *A. glutinosa* and *F. angustifolia*. The Wilcoxon test is used to look for left and right angles for which the maximum sill means are statistically different.

	Cross Section Number	Right Degrees	p-value	Left Degrees	p-value	*A*
A. glutinosa	177	30°	0.0004	15°	0.0029	160°
	225	35°	0.0004	-	-	300°
	273	20°	0.0058	10°	0.0451	245°
	321	20°	0.0808	15°	0.0808	-
	369	15°	0.0022	20°	0.0068	125°
	440	10°	0.0294	5°	0.0767	155°
	473	5°	0.0247	5°	0.0502	100°
	500	40°	0.0001	5°	0.0502	-
	532	10°	0.0127	20°	0.0142	-
F. angustifolia	119	10°	0.031	15°	0.002	40°
	150	10°	0.032	10°	0.032	60°
	204	20°	0.053	10°	0.057	135°
	258	10°	0.77	10°	0.133	115°
	312	10°	0.031	15°	0.002	60°

2009a, 2009b). As the extraction of cores from the overgrowing callus needs to be effected at the contact of the injured and the non-injured tissue, normally more than one sample has to be taken to obtain adequate core samples (Stoffel and Bollschweiler 2008). This means that dendrogeomorphologists have to decide the number of samples required (Stoffel *et al.* 2013) and where to sample by looking at the tree from outside (bark damaged zone). At the same time they cannot move too far from the scar to ensure that the core registers flood damage in the wood structure. The results previously presented are relevant to solving the difficulties in dendrogeomorphic sampling mentioned above.

In the case shown in Figure 4, the internal scanned scar suggests that samples affected by flood impacts can be taken 15° and 35° away from the affected bark, to the right and left, respectively. Variogram results, however, show that density changes are present even further away: 40° and 35° more to the right and left, respectively. Consequently, the study performed for the two selected trees improves the dendrogeomorphic sampling in two important aspects:

- Directed sampling: samples have to be taken from the part of the tree where the wound signal is not attenuated. For the case described in Figure 3, the cores should be sampled in direction c or within the angular sector between directions b and d. The angular sector depends on the species. For the specimens analyzed here, this angular sector can be 181° (*A. glutinosa)* or 82° (*F. angustifolia)*. The measured damage from the scar border for *A. glutinosa* runs from 20° to 12°, to the right and left, respectively, whereas for *F. angustifolia* the affected area is 12° for both left and right sides of the wound.
- Limited sample size (*i.e.* number of trees sampled): this can be reduced depending on the success of the characterization of the flood event with the directed sampling. Hence, less time and effort is needed, not only in the field, but also in processing and interpreting the results.

To sum up, the improvement and extension of these analyses with more specimens and species enables optimal and more efficient sampling. Areas with a low number of injured trees are often discarded for dendrogeomorphic methods or exhaustive sampling is required. Applying this technique means that these zones can be reconsidered for dendrogeomorphic studies.

CONCLUSIONS

A novel methodology was developed and applied to two stems of *F. angustifolia* and *A. glutinosa* seriously damaged by past flash floods.

These samples were scanned with XRCT and external and internal scars were visually located in the scanned images. Using the XRCT technique has the advantage of systematic studying the damage area for each species. The methodology results in a quantitate approximation of this area, for different conditions as health and dimension of the tree, and being much faster than with classical histologic techniques. A number of representative cross-sections were chosen and sample pixel grey-level values were obtained in profiles from the pith to the bark sweeping 360°. For each profile experimental variograms were computed and maximum sills near the origin were recorded. The variograms presented different behaviors (cyclicity, non-stationarity or anisotropy). The flood damage in the wood structure was linked to changes in the variogram sill (zonal anisotropy) and in some cases to the lack of cyclicity. In this study, the moisture content was not distinguished from density variations during XRCT analysis. This hypothesis leads to slightly overestimated wood densities. A refinement of the image analysis procedure could solve this problem in future studies.

Finally, the angular distance of affection A was calculated for each cross-section by using the Wilcoxon test to observe statistical differences in the sill values. Analyses of the A estimations revealed that the area of wood density changes may be much wider than the identifications made visually on the scanned images. Moreover, comparing different A values allowed quantitative classification of the degree of impact affection on the tree. However, further research is needed to relate A values quantitatively with the damaged tree physiology to improve our understanding of post-flood wood response.

This novel methodology clearly helps the automated characterization of the areas within the stem affected by the flash flood impact and represents an advance in research into using XRCT in the study of wood structures. Its application will also improve the systematic acquisition of dendrogeomorphic data with increment cores. Though this work was restricted to two species, its low time-consumption will lead to the study of other species resulting in more general sampling guidelines.

ACKNOWLEDGMENTS

The authors would like to acknowledge the financial support provided by the Spanish Ministry of Economy and Competitiveness in the MAS Dendro-Avenidas Project (CGL2010-19274). We would also like to thank the TRAGSA technicians for their essential support during field work, and other members of the MAS Dendro-Avenidas project, especially Virginia Ruiz-Villanueva and Jose María Bodoque.

REFERENCES CITED

Abràmoff, M., P. Magalhães, and S. Ram, 2004. Image processing with ImageJ. *Biophotonics International* 11(7): 36–42.

Arbellay, E., M. Stoffel, and M. Bollschweiler, 2010. Wood anatomical analysis of *Alnus incana* and *Betula pendula* injured by a debris-flow event. *Tree Physiology* 30(10): 1290–1298.

Arbellay, E., P. Fonti, and M. Stoffel, 2012. Duration and extension of anatomical changes in wood structure after cambial injury. *Journal of Experimental Botany* 63(8): 3271–3277.

Arbellay, E., M. Stoffel, E. K. Sutherland, K. T. Smith, and D. A. Falk, 2014. Changes in tracheid and ray traits in fire scars of North American conifers and their ecophysiological implications. *Annals of Botany* 114(2):223–232.

Armstrong, M., 1984. Problems with universal kriging. *Mathematical Geology* 16(1):101–108.

———, 1998. *Basic linear geostatistics*. Springer-Verlag, Berlini Heidelberg; 153 pp.

Ballesteros-Canovas, J., M. Stoffel, M. Bollschweiler, J. Bodoque, and A. Díez-Herrero, 2010a. Flash-flood impacts cause changes in wood anatomy of *Alnus glutinosa*, *Fraxinus angustifolia* and *Quercus pyrenaica*. *Tree Physiolophy* 30(6): 773–781.

Ballesteros-Canovas, J. A., M. Stoffel, J. Bodoque del Pozo, M. Bollschweiler, O. M. Hitz, and A. Diez-Herrero, 2010b. Changes in wood anatomy in tree rings of *Pinus pinaster* Ait. following wounding by flash floods. *Tree-Ring Research* 66: 93–103.

Benson-Cooper, D., R. Knowles, and F. Thomson, 1982. *Computed tomographic scanning for the detection of defects within logs*. Forest Research Institute, New Zealand Service, Bulletin 8; 9 pp.

Bhandarkar, S., T. Faust, and M. Tang, 1999. Catalog: a system for detection and rendering of internal log defects using computer tomography. *Machine Vision & Applications* 11(4): 171–190.

Castell, W., S. Schrödl, and T. Seifert, 2005. Volume interpolation of CT images from tree trunks. *Plant Biology* 7(6):737–744.

Chang, S., 1990. NMR application for internal defect detection. In: *Proceedings of Process Control/Production Management of Wood Products: Technology for the 90s*. Athens, Georgia.

Chica-Olmo, M., and F. Abarca-Hernández, 2000. Computing geostatistical image texture for remotely sensed data classification. *Computers & Geosciences* 26(4):373–383.

Chilès, J., and P. Delfiner, 2008. *Geostatistics: Modeling Spatial Uncertainty*. Wiley Online Library; 720 pp.

Deutsch, C., and A. Journel, 1992. *Gslib: Geostatistical Software Library and User's Guide*. Oxford University Press, New York, 1992; 340 pp.

Fan, Z. X., A. Bräuning, Y. Bao, and K. F. Cao, 2009. Tree ring density-based summer temperature reconstruction for the central Hengduan Mountains in southern China. *Global Planetary Change* 65:1–11.

Fonti, P., N. Solomonoff, and I. García-González, 2007. Earlywood vessels of *Castanea sativa* record temperature before their formation. *New Phytologist* 173(3):562–70.

Freyburger, C., F. Longuetaud, F. Mothe, T. Constant, and J. Leban, 2009. Measuring wood density by means of x-ray computer tomography. *Annals of Forest Science* 66:804.

Fritts, H. C., 1976. *Tree Rings and Climate*. Academic Press, London; 567 pp.

Funt, B., and E. Bryant, 1985. A computer vision system that analyzes CT-scans of sawlogs. In: *Proceedings of IEEE Conference on Computer Vision and Pattern Recognition*, pp. 175–177. San Francisco, California.

———, 1987. Detection of internal log defects by automatic interpretation of computer tomography images. *Forest Products Journal* 37(1):56–62.

García Esteban, L., A. Guindeo Casasus, C. Peraza Oramas, and P. de Palacios, 2003. *La madera y su anatomía: anomalías y defectos, estructura microscópica de coníferas y frondosas, identificación de maderas, descripción de especies y pared celular*. Mundi-Prensa Libros; 327 pp.

Garcia-Gonzalez, I., and P. Fonti, 2006. Selecting early vessel to maximize their environmental signal. *Tree Physiology* 26: 1289–1296.

Goovaerts, P., 1997. *Geostatistics for Natural Resources Evaluation*. Oxford University Press, USA; 483 pp.

Hodges, D., W. Anderson, and C. McMillin, 1990. The economic potential of CT scanners for hardwood sawmills. *Forest Production Journal* 40(3):65–69.

Isaaks, E., and R. Srivastava, 1989. *Applied Geostatistics*. Oxford University Press; 561 pp.

Journel, A., and C. Huijbregts, 1978. *Mining Geostatistics, Vol. 859*. Academic Press, New York; 600 pp.

Leban, J., A. Pizzi, S. Wieland, M. Zanetti, M. Properzi, and F. Pichelin, 2004. X-ray microdensitometry analysis of vibration-welded wood. *Journal of Adhesion Science and Technology* 18(6):673–685.

Longuetaud, F., 2005. *Détection et Analyse Non Destructive de Caractéristiques Internes de Billons D'epicéa Commun (*Picea abies *(l.) karst.) par Tomographie à Rayons x*. Ph.D. thesis, ENGREF (AgroParisTech).

Longuetaud, F., L. Saint-André, and J. Leban, 2005. Automatic detection of annual growth units on *Picea abies* logs using optical and x-ray techniques. *Journal of Nondestructive Evaluation* 24(1):29–43.

Matheron, G., 1965. *Les Variables Régionalisées et Leur Estimation: Une Application de la Théorie des Fonctions Aléatoires aux Sciences de la Nature*. Masson Paris, France; 305 pp.

Olea, R. A., 1994. Fundamentals of semivariogram estimation, modeling, and usage. In: *CA 3: Stochastic Modeling and Geostatistics*, edited by J. M. Yarus, and R. L. Chambers, pp. 27–35. American Association of Petroleum Geology Special Volume, Tulsa, Oklahoma.

Roder, F., E. Scheinman, and P. Magnuson, 1989. High-speed CT scanning of logs. In: *Proceedings of the 3rd International Conference on Scanning Technology in Sawmilling;* pp VI, pp. 1–9. Oct. 5–6 Oakland, CA.

Romero, C., B. M. Bolker, and C. E. Edwards, 2009. Stem responses to damage: the evolutionary ecology of Quercus species in contrasting fire regimes. *New Phytologist* 182:261–271.

Schinker, M., N. Hansen, and H. Spiecker, 2003. High-frequency densitometry - A new method for the rapid evaluation of wood density variations. *IAWA Journal* 24(3): 231–239.

Schneuwly, D. M., M. Stoffel, and M. Bollschweiler, 2009a. Formation and spread of callus tissue and tangential rows of resin ducts in *Larix decidua* and *Picea abies* following rockfall impacts. *Tree Physiology* 29:281–289.

Schneuwly, D. M., M. Stoffel, L. K. A. Dorren, and F. Berger, 2009b. Three-dimensional analysis of the anatomical growth response of European conifers to mechanical disturbance. *Tree Physiology* 29:1247–1257.

Schweingruber, F., A. Börner, and E. Schulze, 2006. *Atlas of Woody Plant Stems: Evolution, Structure, and Environmental Modifications*. Springer-Verlag, Berlin; 229 pp.

Shigo, A., 1984. Compartmentalization: a conceptual framework for understanding how trees grow and defend themselves. *Annual Review of Phytopathology* 22(1):189–214.

Smith, K. T., and E. K. Sutherland, 1999. Fire scar formation and compartmentalization in oak. *Canadian Journal of Forest Research* 29:166–171.

Stoffel, M., and M. Bollschweiler, 2008. Tree-ring analysis in natural hazards research – An overview. *Natural Hazards & Earth System Sciences* 8:187–202.

Stoffel, M., and O. M. Hitz, 2008. Snow avalanche and rockfall impacts leave different anatomical signatures in tree rings of *Larix decidua*. *Tree Physiology* 28(11):1713–1720.

Stoffel, M., and M. Bollschweiler, 2010. Tree-ring analysis in natural hazards research – Preface. *Natural Hazards & Earth System Sciences* 10:2355–2357.

Stoffel, M., M. Bollschweiler, D. R. Butler, and B. H. Luckman, 2010. *Tree rings and natural hazards: A state-of-the-art*. Springer, Berlin, Heidelberg, New York; 505 pp.

Stoffel, M., and M. Klinkmüller, 2013. 3D analysis of anatomical reactions in conifers after mechanical wounding: first qualitative insights from X-ray computed tomography. *Trees*. doi: 10.1007/s00468-013-0900-2.

Stoffel, M., D. R. Butler, and C. Corona, 2013. Mass movements and tree rings: A guide to dendrogeomorphic field sampling and dating. *Geomorphology*. doi: 10.1016/j.geomorph.2012.12.017.

Van den Bulcke, J., E. L. G. Wernersson, M. Dierick, D. V. Loo, B. Masschaele, L. Brabant, M. N. Boone, L. Van Hoorebeke, K. Haneca, A. Brun, C. L. L. Hendriks, and J. Van Acker, 2014. 3D tree-ring analysis using helical X-ray tomography. *Dendrochronologia* 32:39–46.

Wagner, F., F. Taylor, D. Ladd, C. McMillin, and F. Roder, 1989. Ultrafast CT scanning of an oak log for internal defects. *Forest Products Journal* 39(11/12):62–64.

Webster, R., and M. Oliver, 2007. *Geostatistics for Environmental Scientists*. Wiley, West Sussex, England.

Wilcoxon, F., 1945. Individual comparisons by ranking methods. *Biometrics Bulletin* 1(6):80–83.

Received 3 January 2014; accepted 10 August 2014.